

Fractal structure of bubbston clusters in water and aqueous electrolytic solutions

N. F. Bunkin and A. V. Lobehev

Institute of General Physics, Russian Academy of Sciences, 117924 Moscow, Russia

(Submitted 21 May 1993)

Pis'ma Zh. Eksp. Teor. Fiz. **58**, No. 2, 91–97 (25 July 1993)

Experiments confirm that clusters of microscopic bubbles (bubbston clusters) arise in a liquid as the result of a coagulation of elementary microbubbles (bubbstons). Their fractal dimension and average radius have been determined for water and for aqueous solutions of electrolytes and coagulants. The fractal properties of the clusters depend on the concentration of the electrolyte. It is shown experimentally that there is a relationship between the threshold for optical breakdown in a liquid and the number density of clusters.

It was first suggested in Ref. 1 that a gas dissolved in a liquid might lead to the formation of microscopic gas bubbles which are stable in time and which are capable of combining into clusters. A theory of a “bubbston”-cluster structure of liquids was derived in a subsequent paper.² It was shown that the presence of even extremely tiny traces of an electrolyte (i.e., ions) in a liquid (with a dissolved gas) leads to the spontaneous appearance of stable gas bubbles called “bubbstons” (from “bubbles stabilized by ions”). In pure water, the required concentration of ions is provided by the electrolytic dissociation of the water molecules themselves, and the radius of a bubbston, R_0 , is ~ 100 Å. It was also established that a Brownian diffusion of bubbstons should be accompanied by their coagulation, resulting in the formation of clusters. Since bubbston clusters form as the result of a diffusion-controlled aggregation, it can be concluded (Refs. 3–5, for example) that the clusters which form in such a process are fractals: entities of noninteger dimensionality. Ideas concerning bubbston clusters have made it possible to take a fresh look at the physical nature of such superficially diverse effects as cavitation and laser breakdown of liquids⁶ and to develop a new quantitative interpretation of experimental data. On the other hand, no experimental data have been found which would directly confirm the existence of a bubbston-cluster structure of liquids. In the present letter we present some corresponding data, for pure water and for aqueous electrolytic solutions. We show that the scattering of light by these liquids has the standard characteristics of scattering by fractal structures in which the dimensions of the monomers (the colloidal particles) are small in comparison with the wavelength of the light.⁷ The size of these structures is on the order of tens of microns and depends on the coagulation properties of the liquid. A change in the number of these structures per unit volume affects the threshold for optical breakdown; i.e., they can be associated with bubbston clusters.

The cross section for the scattering of unpolarized light in a unit volume of a liquid colloidal solution of identical gas bubbles of radius R_0 can be written

$$d\sigma/d\Omega = (k^4/2)(1 + \cos^2\theta) \{ (\rho \partial n^2 / \partial \rho)^2 \beta_T T / 16n^2 + [(n^2 - 1)/(2n^2 + 1)]^2 R_0^6 N(1 + S(q)) \}. \quad (1)$$

Here $k = 2\pi/\lambda$, $q = (4\pi/\lambda)\sin\theta/2$ (λ is the wavelength of the light); θ is the scattering angle; n , T , ρ , and β_T are, respectively, the refractive index, temperature, density, and compressibility of the liquid (the solvent); and $N = \langle N(r) \rangle$ is the average number density of bubbles. The structure factor is defined by

$$S(q) = 4\pi N \int_0^\infty G(r) (\sin qr / qr) r^2 dr, \quad (2)$$

where $G(r) = [\langle N(\mathbf{r}')N(\mathbf{r}'+\mathbf{r}) \rangle / N^2] - 1$ is the correlation function in the relative positions of the bubbles. The first term in (1) corresponds to "classical" molecular scattering of light (Ref. 8, for example), and the two-part second term corresponds to Rayleigh scattering by small particles (the gas bubbles). The first part of the second term does not depend on the structure of the arrangement of bubbles. It corresponds to an incoherent scattering (the intensities of the scattering by the individual bubbles are summed). The second part, which is proportional to $S(q)$, describes a coherent scattering due to the presence of a certain (average) structure in the arrangement of bubbles in the solution. Numerical estimates show that in water under standard conditions, with bubble radii $R_0 \sim 10^2 \text{ \AA}$ and a bubble number density $N \sim 10^{12} \text{ cm}^{-3}$ (Refs. 2 and 3), the molecular scattering and the incoherent part of the scattering by bubbles are comparable in magnitude. They create the scattering background against which we were to distinguish the contribution from the bubble-cluster structure of the liquid in our experiments.

It is easy to find the value of the function $G(r)$ at $r < a$ and $r > R_c$, where a is the closest distance to which individual bubbles can approach each other in a cluster, and R_c is the average radius of the clusters. According to Ref. 2, a bubble consists of a core—a stable gas bubble of radius R_0 —surrounded by an ion sheath of radius a_0 . For electrolytic solutions which are not too highly concentrated, the radius a_0 is the Debye length $a_D = (\epsilon T / 8\pi e^2 n_i)^{1/2}$ (ϵ is the dielectric constant of the liquid, and n_i is the density of ions). In particular, for pure water we would have $a_0 = a_D \approx 2 \times 10^{-5}$ cm. It was also shown in Ref. 2 that, when the ion sheaths of two bubble clusters overlap, the minimum distance is $a = 2a_0 = 2a_D \approx 4 \times 10^{-5}$ cm (in the case of water). At $r < a$, we obviously have an average value $\langle N(\mathbf{r}')N(\mathbf{r}'+\mathbf{r}) \rangle = 0$. We thus have $G(r) = -1$. At $r > R_c$, at least one of the points $(\mathbf{r}'+\mathbf{r})$ and \mathbf{r}' is outside the cluster, so the fluctuations in the density of bubbles at these two points are statistically independent. We then have $\langle N(\mathbf{r}'+\mathbf{r})N(\mathbf{r}') \rangle = N^2$. We thus find the result $G(r) = 0$ at $r > R_c$ (we can assume that the radius of a cluster, R_c , is the correlation radius for the correlation in the bubble density fluctuations). The problem of determining the function $G(r)$ in the interval $a < r < R_c$ falls in the category of problems of the statistical theory of disordered structures. It cannot be solved without invoking models for the structures. For so-called massive fractals, for which the number (or "mass" M) of the colloidal particles (bubbles in the case at hand) is related to the fractal dimensionality D by $M \propto R_c^D$ (structures of the polymer type), the function $G(r)$ is (Refs. 9 and 10, for example)

$$G(r) \sim r^{D-3}, \quad a < r < R_c. \quad (3)$$

According to Ref. (2), the structure factor $S(q)$ is governed primarily by specifically this interval of r values, since the integration over the interval $(0, a)$ in (2) (in which we have $G = -1$) gives us $(-4\pi/3)a^3N$. This quantity is (first) independent of q and (second) small in comparison with the one in (1). Substituting (3) into (2), we find

$$S(q) \sim q^{-D} \int_{aq}^{R_c q} x^{D-2} \sin(x) dx.$$

For small-angle scattering, with $aq \ll 1$, but $R_c q \gg 1$ (the latter condition can hold since the ratio R_c/a is very large), the integral in this formula is independent of q within terms $\sim (aq)^{D-1}$, so we have

$$S(q) \sim q^{-D}, \quad R_c^{-1} < q < a^{-1}. \quad (4)$$

The half-width of the scattering angle, $\Delta\theta$ (at the level of half the maximum intensity), which is given, in general, by the formula

$$\Delta\theta = (\lambda/2\pi) \left[3 \int_a^{R_c} r^2 G(r) dr / \int_a^{R_c} r^4 G(r) dr \right]^{1/2},$$

turns out to be

$$\Delta\theta = (\lambda/2\pi R_c) [3(2+D)/D]^{1/2}. \quad (5)$$

A q dependence of the factor $S(q)$ as in (4) is known to be characteristic of small-angle scattering (of light, x radiation, and neutrons) by all disordered structures: $S(q) \propto q^{-k}$, where k is the Porod index. This index can take on a wide range of positive values, depending on the type of structure.⁹

Figure 1 shows the experimental layout for our study of small-angle scattering. We used the beam from a Xe-Cl excimer laser ($\lambda = 308$ nm, pulse length of 10 ns) or the second harmonic of a neodymium laser ($\lambda = 532$ nm, pulse length of 15 ns) operating on a single transverse mode. The laser beam was sent through a system of diaphragms [the first provided diffraction rings; a second (an iris diaphragm) transmitted only the main lobe of the radiation] to the cell holding the test liquid. This cell consisted of a cylindrical quartz cup of radius $R = 3$ cm (the exit window), cut in half along a generatrix. A plane quartz entrance window was cemented to the cup. We suppressed highlights in the interference pattern due to rereflections from the front and rear walls of the entrance and exit windows by making these windows in the form of optical wedges (respectively, planar and cylindrical). The test liquid was poured into the vertically positioned cell, and the cell became a cylindrical lens. Its focal length (measured from the entrance window) was $f = Rn/(n-1)$, where n is the refractive index of the liquid. The distance f was determined experimentally for each wavelength. Photographic film was mounted along a semicircle of radius f in the horizontal plane of the laser beam in order to record the scattered light. The photographs were then studied on a densitometer.

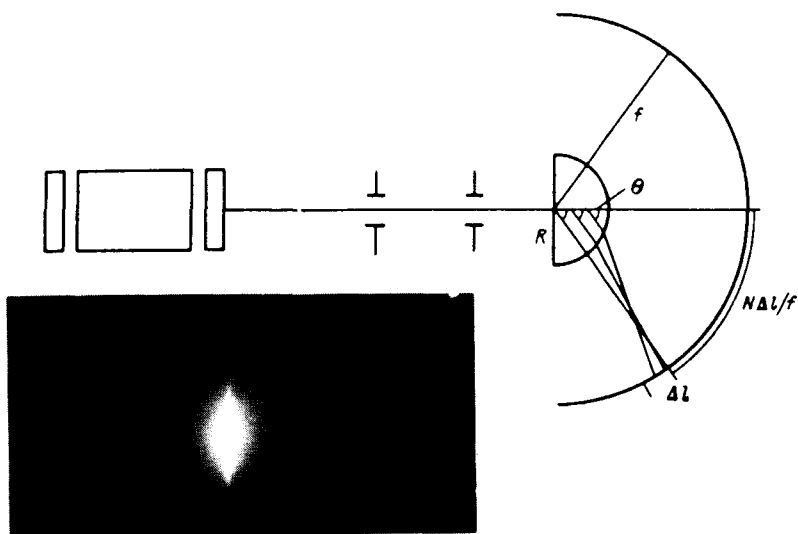


FIG. 1. Experimental layout.

The photographs of the scattered signal were analyzed by the following procedure. The position of the laser spot on the film, which was clearly distinguishable against the background of scattered light (see the inset in Fig. 1), was adopted as the origin of coordinates. Densitometer traces were recorded at steps $\Delta x = 0.5$ mm along the film. The angle $N\Delta x/f$ (N is the index of the step) corresponding to each point on the densitometer trace was identified with the scattering angle θ in the liquid. We know that at small angles θ there are no aberrations resulting from a distribution of scattering entities along the incident beam (within a radius R ; this assertion holds within the approximation of $\sin\theta$ by θ), so the equality $\theta = N\Delta x/f$ holds (according to our estimates in the geometric-optics approximation, for the value $\theta = 20^\circ$ the width of the aberration spot on the film is only $\Delta l = 0.3$ mm, and it decreases rapidly with decreasing θ). This layout has the advantage that (first) the transmitted light can be effectively separated from the light scattered at small angles. Second, the far zone (the observation zone) is determined by the distance f for the entire angular spectrum of the scattered light. The apparatus can thus be made quite compact. Since the unscattered light is localized very sharply in the focus, we can "approach" the laser spot quite closely in the densitometry. We should mention that dust particles and a roughness on the optical elements create very serious obstacles to attempts to achieve a high resolution.

The liquids which were studied were distilled water and aqueous solutions of MgCl_2 , $\text{Al}_2(\text{SO}_4)_3$, KOH , and alumoammonium alum with a concentration of 0.1 M and an aqueous solution of polyacrylamide with a concentration of 10^{-4} M. Before being poured into the cell, the liquids were filtered. After being poured into the cell, they were left to stand for a day before an experiment.

In the densitometry we determined the scattering function $S(\theta)$ (we did not

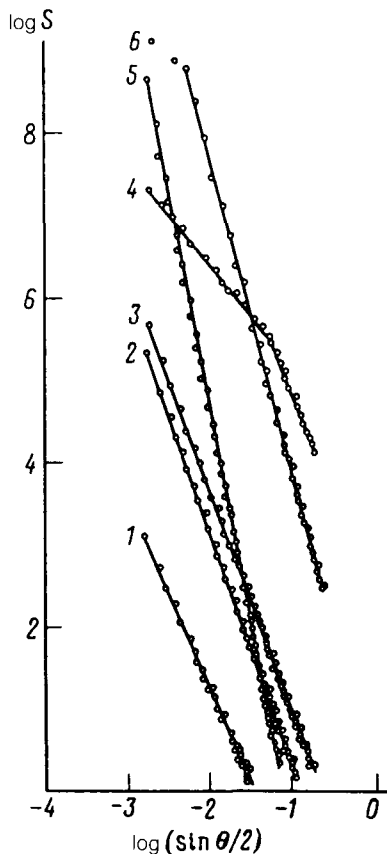


FIG. 2. $\log S$ (in arbitrary units) versus $\log(\sin\theta/2)$. 1—Water, $k=2.1$; 2— MgCl_2 solution, $k=2.4$; 3— $\text{Al}_2(\text{SO}_4)_3$ solution, $k=2.38$; 4—KOH solution, $k_1=1.13$, $k_2=2.32$; 5—alumoammonium alum solution, $k=4.5$; 6—polyacrylamide solution, $k=3.4$.

carry out a densitometer study of the region on the film corresponding to the focused laser beam, with an angular size $\approx 0.5^\circ$). We then determined the area under the $S(\theta)$ curve—the total scattered energy S_0 —and the angular width of the function at half-maximum, $\Delta\theta$. As the maximum value S_{\max} we used the value corresponding to the smallest measurable scattering angle, $\Delta x/f$, so the values of $\Delta\theta$ measured in this manner should be regarded as being on the high side. We also measured $\log S$ as a function of $\log q = \log[(4\pi/\lambda)\sin\theta/2]$. Figure 2 shows this functional dependence for the liquids studied for the wavelength $\lambda = 308$ nm (some differences in these results for the case $\lambda = 532$ nm are pointed out below). For all the liquids studied (except the KOH solution) the function is a straight line with a negative slope (the slope—the Porod index—is shown in Fig. 2). It can be seen from Fig. 2 that in the case of the polyacrylamide solution several points corresponding to scattering angles near 0° do not conform to a straight line. The probable reason is an error in the densitometry due to saturation of the film by the overly intense scattered light in this case. At $\lambda = 532$ nm we have $k=3$ for this solution. This discrepancy in the values of k for the two λ 's is observed for only this solution. It may be due to a violation of condition (4) for the polyacrylamide solution. It can also be seen from Fig. 2 that for the KOH solution

there is a crossover near an angle of 10° : As θ increases, the straight line with a negative slope $k_1=1.13$ converts into one with $k_2=2.32$. At $\lambda=532$ nm, the position of the crossover corresponds to an angle of 5.7° , and the negative slopes are $k_1=1.09$ and $k_2=2.26$. The ratio of the crossover angles is close to the ratio of wavelengths, and the ratios k_1/k_2 are approximately the same. The crossover may be due to the presence of two correlation radii for correlations in the fluctuations of the density $[N(r)]$ of bubbstons in a cluster. We carried out an experiment as a check: We replaced the cell holding the liquid by a cylindrical quartz lens with the same focal length, and we measured $\log S$ as a function of $\log q$. In the angular interval $20^\circ \geq \theta \geq 0.9^\circ$ we observed no dependence (i.e., we found $k=0$). At $\theta < 0.9^\circ$ we observed a significant change in the slope; the coefficients k were sharply different for both λ 's in this case. This scattering is apparently due to defects in the optical elements.

We can work from the measured values of $\Delta\theta$ and (5) to estimate the dimensions of the scattering fractal clusters. This estimate of R_c should be regarded as only approximate, since it is not always the same for the wavelengths used. The error stems from the arbitrariness in the determination of the maximum value S_{\max} (see the discussion above). Knowing k for a given liquid, we can determine S_{\max} at $\theta=0^\circ$ by computer extrapolation. The values found for $\Delta\theta$ for the two λ 's in this manner are approximately the same, so we will report the results for $\lambda=308$ nm to illustrate the general trends in the behavior of R_c . For water we find $R_c \approx 28 \mu\text{m}$. For the MgCl_2 solution we find $R_c \approx 33 \mu\text{m}$; for the KOH solution we find $\approx 39 \mu\text{m}$; for the $\text{Al}_2(\text{SO}_4)_3$ solution we find $\approx 58 \mu\text{m}$; and for the polyacrylamide and alumoammonium solutions we find $\approx 12 \mu\text{m}$. The increase in R_c in the electrolytic solutions can be explained on the basis of the familiar tendency (Ref. 11, for example) of electrolytic salts to lower the coagulation barrier for particles. This effect should lead to an increase in the size of particles during coagulation.

The experimental values found for the Porod index k lead to the conclusion that bubbston clusters in distilled water and also in aqueous solutions of MgCl_2 and $\text{Al}_2(\text{SO}_4)_3$ are massive fractals with dimensionalities $D=2.1, 2.4$, and 2.38 , respectively. For the clusters in the aqueous solutions of KOH, the alumoammonium alum, and the polyacrylamide, all that we can say is that their disordered structure differs from that of massive fractals.

In conclusion we would also like to point out that the total scattering energy S_0 is proportional to the number of clusters per unit volume of the liquid. As this density increases, according to Ref. 3, the threshold for laser breakdown of the liquid decreases. The ratio of S_0^w , for water and the corresponding energy for a solution at a given concentration, S_0^s (i.e., the quantity S_0^w/S_0^s), can be compared with the ratio of breakdown thresholds, $I_{\text{th}}^s/I_{\text{th}}^w$, in these liquids (I_{th} is the threshold intensity). Stopping shy of a quantitative analysis of these quantities, we would point out that they behave similarly, i.e., fall off sharply, with increasing concentration of the solution.

We wish to thank F. V. Bunkin and G. A. Lyakhov for useful discussions of this study.

¹N. F. Bunkin and V. B. Karpov, JETP Lett. **52**, 18 (1990).

²N. F. Bunkin and F. V. Bunkin, **101**, 512 (1992) [Sov. Phys. JETP **74**, 271 (1992)].

- ³T. A. Witten and L. M. Sander, *Phys. Rev.* **B27**, 493 (1983).
⁴P. Meakin, *Phys. Rev. Lett.* **51**, 1119 (1983); *J. Chem. Phys.* **81**, 4637 (1984).
⁵T. Viscek, *Phys. Rev. Lett.* **53**, 2281 (1984).
⁶N. F. Bunkin and F. V. Bunkin, *Laser Phys.* **3**, 63 (1993).
⁷J. Feder, *Fractals*, Plenum, New York, 1988.
⁸I. L. Fabelinskiĭ, *Molecular Scattering of Light* (Nauka, Moscow, 1965).
⁹D. W. Schaefer and K. D. Heefer, *Proceedings of the Sixth Trieste International Symposium on Fractals in Physics* (Italy, 1985).
¹⁰D. W. Schefer, J. E. Martin, P. Wiltzius, and D. S. Canell, *Phys. Rev. Lett.* **52**, 2371 (1984).
¹¹Yu. G. Frolov, *Course in Colloidal Chemistry* (Khimiya, Moscow, 1982).

Translated by D. Parsons